DEVELOPMENT OF A DYNAMIC MULTI-COMPARTMENT MODEL FOR THE PREDICTION OF PARTICLE SIZE DISTRIBUTION AND MOLECULAR PROPERTIES IN A CATALYTIC OLEFIN POLYMERIZATION FBR

G. Dompazis, V. Kanellopoulos and C. Kiparissides,

*Department of Chemical Engineering and Chemical Process Engineering Research Institute,
Aristotle University of Thessaloniki, P.O. Box 472, Thessaloniki, Greece 541 24*

Abstract: In the present study a comprehensive multi-compartment model is developed for the prediction of particle size distribution and particle segregation in a catalytic olefin polymerization FBR. To calculate the particle growth and the spatial monomer and temperature profiles in a particle, the random pore polymeric flow model (RPPFM) is utilized. The RPPFM is solved together with a dynamic discretized particle population balance model, to predict the particle size distribution (PSD) in each compartment. In addition, the polymer molecular properties are calculated, in each reactor compartment, by employing a generalized multi-site, Ziegler-Natta, kinetic scheme. The effects of various fluidized bed operating conditions on the morphological and molecular distributed polymer properties are thoroughly analyzed. *Copyright © 2006 IFAC*

Keywords: Polymerization, particle size measurement, modeling

1. INTRODUCTION

High and low density polymers are commercially manufactured in gas phase fluidized bed olefin polymerization reactors using high activity transition metal catalysts such as Ziegler-Natta catalysts, Phillips-Chromium oxide catalysts and supported metallocene catalysts. Although polymer particles are assumed to be very well-mixed, particle segregation may occur in large industrial fluidized bed reactors. This means that the polymer particle size distribution at the reactor exit may differ from the PSDs at different locations along the reactor height. In a fluidized bed reactor strong segregation can occur if the bed contains particles of different densities. Density differences are a common reason for particle segregation but particle size differences can also cause it.

Despite its inherent importance, a limited number of papers have been published on the modeling of the particle-size distribution in gas-phase catalytic olefin polymerization processes. Zacca, et al. (1994), developed a population balance model using the catalyst residence time as the main coordinate, to model particle-size developments in multistage olefin polymerization reactors, including vertical and horizontal stirred beds and fluidized-bed reactors. Choi, et al. (1994), incorporated an isothermal simplified multigrain particle model, by neglecting the external particle mass and heat transfer resistances, into a steady-state PBE to investigate the effect of catalyst deactivation on the PSD and average molecular properties for both uniform and size distributed catalyst feeds. Yiannoulakis, et al. (2001), extended the model of Choi, et al. (1994), to account for the combined effects of internal mass and heat transfer resistances on the PSD for highly active catalysts. In a recent publication Dompazis, et al. (2005), developed a comprehensive integrated model, accounting for the multi-scale phenomena taking place in a continuous gas-phase ethylene copolymerization FBR to describe the molecular and morphological properties of the particulate polymer. Kim and Choi, (2001) presented a steady state multi-compartment population balance model using the concept of size-dependent absorption/spillage model to investigate the effects of fluidization and reaction conditions on the reactor performance.

In what follows, a dynamic multi-compartment model is developed for the prediction of morphological and molecular distributed polymer properties in an FBR.

2. POLYMERIZATION KINETIC MODEL

To describe the molecular weight developments over a heterogeneous Ziegler-Natta catalyst, a generalized two-site kinetic model is employed (Table 1) (Hatzantonis et al., 2000). The kinetic mechanism comprises of a series of elementary reactions, including site activation, propagation, site deactivation and site transfer reactions. The symbol $P_{n,i}^k$ denotes the concentration of "live" copolymer chains of total length 'n' ending in an 'i' monomer unit, formed at the 'k' catalyst active site. P_0^k and D_n^k denote the concentrations of the activated vacant catalyst sites of type 'k' and "dead" copolymer chains of length 'n' produced at the 'k' catalyst active site, respectively.

Table 1 Kinetic mechanism of ethylene-propylene copolymerization over a Ziegler-Natta catalyst.

Activation by aluminum alkyl:	$S_p^k + A \xrightarrow{k_{aA}^k} P_0^k$
Chain initiation:	$P_0^k + M_i \xrightarrow{k_{0,i}^k} P_{1,i}^k$
Propagation:	$P_{n,i}^k + M_j \xrightarrow{k_{p,ij}^k} P_{n+1}^k$
Spontaneous deactivation:	$P_*^k \xrightarrow{k_{dsp}^k} C_d^k + D_n^k$
Chain transfer by hydrogen (H_2):	$P_{n,i}^k + H_2 \xrightarrow{k_{tH,i}^k} P_0^k + D_n^k$

Based on the postulated kinetic mechanism one can define the "live" (λ_ν) and "bulk" (ξ_ν) moments with respect to the corresponding total number chain length distributions (TNCLDs). The average polymer properties of interest (i.e., number and weight average molecular weights) can be calculated.

Number-average molecular weight:

$$M_n = \left(\sum_{k=1}^{N_s} \xi_1^k \Big/ \sum_{k=1}^{N_s} \xi_0^k \right) \sum_{k=1}^{N_s} MW^k \qquad (1)$$

Weight-average molecular weight:

$$M_w = \left(\sum_{k=1}^{N_s} \xi_2^k \Big/ \sum_{k=1}^{N_s} \xi_1^k \right) \sum_{k=1}^{N_s} MW^k \qquad (2)$$

where MW^k is the average molecular weight of the repeating unit in the copolymer chains.

$$MW^k = \sum_{i=1}^{N_m} \Phi_i^k MW_i \qquad (3)$$

In the particle level the number- and weight- average molecular weights are diameter-dependent and are obtained by integrating over the particle volume.

Mean-average molecular weights of a polymer particle of size D :

$$M_n(D) = \frac{1}{r} \int_0^{D/2} M_n(r)\,dr \;,\; M_w(D) = \frac{1}{r} \int_0^{D/2} M_w(r)\,dr \quad (4)$$

3. SINGLE PARTICLE GROWTH MODELING

To simulate the growth of a single polymer particle, the random pore polymeric flow model (RPPFM) of Kanellopoulos, et al. (2004), was employed. In the RPPFM, the polymer particle is assumed to be spherical, while the heterogeneous polymer and catalyst phases are treated as a pseudo-homogeneous medium of constant density. Monomer diffusion and heat conduction are assumed to occur only in the radial direction, and diffusion of all the other species (e.g., polymer chains) is considered to be negligible. As a result, the overall monomer transport rate will largely depend on the catalyst/particle morphology, which continuously changes with polymerization time. The equations to be solved for the calculation of spatial ethylene and propylene concentrations and temperature profile in a growing polymer particle, as well as the overall particle polymerization rate are presented elsewhere (Kanellopoulos, et al., 2004).

4. MULTI-COMPARTMENT MODEL

To calculate the dynamic evolution of PSD and particle segregation in a gas-phase fluidized bed reactor a dynamic population balance model needs to be solved together with the system of differential equations describing the radial monomer(s) concentration and temperature profiles in a single particle (Kanellopoulos, et al., 2004). The bed is divided into N equally sized virtual compartments, as illustrated in Figure 1 and each reactor zone consists of a bulk emulsion phase compartment and a wake compartment. Let us assume that the operation of each compartment can be approximated by a perfectly back-mixed, continuous flow reactor. Polymer particles are fed into each compartment from other compartments, while the mass of solids in the compartment is kept constant by controlling the product withdrawal rate.

The dynamic population balance equation and the overall mass balance in each reactor compartment can take the following forms:

Top compartment (n=1)

Bulk Phase:

$$\frac{\partial n_1(D,t)}{\partial t} + \frac{\partial [G(D)n_1(D,t)]}{\partial D} = \frac{1}{W_{b,1}} F_c n_c(D) +$$

$$\frac{1}{W_{b,1}} \left[F_{tr,1}^{wb} n_{tr,1}^{wb}(D,t) + u_{b,1} A_{w,1} \rho_p n_{w,1}(D,t) \right] -$$

$$\frac{1}{W_{b,1}} \left[F_{tr,1}^{bw} n_{tr,1}^{bw}(D,t) + F_1 n_1(D,t) + u_{b,1} A_{w,1} \rho_p n_{w,1}(D,t) \right] \qquad (5)$$

$$W_{b,1} \int_{D_{min}}^{D_{max}} G(D) n_1(D,t) d(\rho_p \pi D^3 / 6) - F_1 + \tag{6}$$

$$u_{b,1} A_{w,1} \rho_p + F_c = 0$$

Wake Phase:

$$\frac{\partial n_{w,1}(D,t)}{\partial t} = \frac{1}{W_{w,1}} \left[u_{b,2} A_{w,2} \rho_p n_{w,2}(D,t) + F_{tr,1}^{bw} n_{tr,1}^{bw}(D,t) \right] - \tag{7}$$

$$\frac{1}{W_{w,1}} \left[u_{b,1} A_{w,1} \rho_p n_{w,1}(D,t) + F_{tr,1}^{wb} n_{tr,1}^{wb}(D,t) \right]$$

$$u_{b,2} A_{w,2} \rho_p - u_{b,1} A_{w,1} \rho_p + F_{tr,1}^{bw} - F_{tr,1}^{wb} = 0 \tag{8}$$

ith compartment (n=i)

Bulk Phase:

$$\frac{\partial n_i(D,t)}{\partial t} + \frac{\partial [G(D) n_i(D,t)]}{\partial D} = \frac{1}{W_{b,i}} \left[F_{i-1} n_{i-1}(D,t) \right] - \tag{9}$$

$$\frac{1}{W_{b,i}} \left[F_i n_i(D,t) - F_{tr,i}^{wb} n_{tr,i}^{wb}(D,t) + F_{tr,i}^{bw} n_{tr,i}^{bw}(D,t) \right]$$

$$F_{i-1} + W_{b,i} \int_{D_{min}}^{D_{max}} G(D) n_i(D,t) d(\rho_p \pi D^3 / 6) - F_i = 0 \tag{10}$$

Wake Phase:

$$\frac{\partial n_{w,i}(D,t)}{\partial t} = \frac{1}{W_{w,i}} u_{b,i+1} A_{w,i+1} \rho_p n_{w,i+1}(D,t) - \tag{11}$$

$$\frac{1}{W_{w,i}} \left[u_{b,i} A_{w,i} \rho_p n_{w,i}(D,t) + F_{tr,i}^{wb} n_{tr,i}^{wb}(D,t) - F_{tr,i}^{bw} n_{tr,i}^{bw}(D,t) \right]$$

$$u_{b,i+1} A_{w,i+1} \rho_p - u_{b,i} A_{w,i} \rho_p + F_{tr,i}^{bw} - F_{tr,i}^{wb} = 0 \tag{12}$$

Bottom compartment (n=i)

Bulk Phase:

$$\frac{\partial n_N(D,t)}{\partial t} + \frac{\partial [G(D) n_N(D,t)]}{\partial D} = \frac{1}{W_{b,N}} F_{N-1} n_{N-1}(D,t) - \tag{13}$$

$$\frac{1}{W_{b,N}} \left[F_N n_N(D,t) + F_{tr,N}^{bw} n_{tr,N}^{bw}(D,t) - F_{tr,N}^{wb} n_{tr,N}^{wb}(D,t) \right] -$$

$$\frac{1}{W_{b,N}} F_{re} n_{re}(D,t)$$

$$W_{N,i} \int_{D_{min}}^{D_{max}} G(D) n_N(D,t) d(\rho_p \pi D^3 / 6) + \tag{14}$$

$$F_{N-1} - F_N - F_{re} = 0$$

Wake Phase:

$$F_{re} - u_{b,N} A_{w,N} \rho_p + F_{tr,N}^{bw} - F_{tr,N}^{wb} = 0 \tag{15}$$
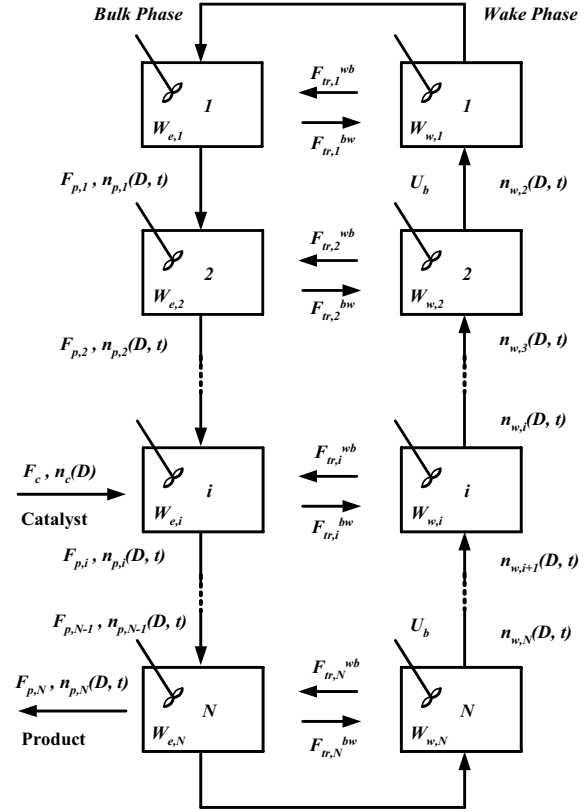
Fig. 1. Schematic representation of the multi-compartment model.

$$\frac{\partial n_{w,N}(D,t)}{\partial t} = \frac{1}{W_{w,N}} \left[F_{re} n_{re}(D,t) + F_{tr,N}^{bw} n_{tr,N}^{bw}(D,t) \right] - \tag{16}$$

$$\frac{1}{W_{w,N}} \left[u_{b,N} A_{w,N} \rho_p n_{w,N}(D,t) + F_{tr,N}^{wb} n_{tr,N}^{wb}(D,t) \right]$$

where $n_i(D,t)$, $n_{w,i}(D,t)$, $n_{re}(D,t)$, expressed in (#/g/cm), denote the number diameter density functions of particles in the bulk phase, in wake phase of compartment i and in the recycle stream respectively. The term $n_i(D,t)dD$ denotes the number of particles in the size range $(D, D + dD)$ per mass of polymer in the bulk phase of compartment i at time t. u_b is the rising bubble velocity and A_w is the effective cross section area of the wake phase

In order to calculate the individual particle growth rate and temperature profile, one has to solve the monomer and energy balances for each discrete class of particles. According to Hatzantonis, et al. (1998), the particle growth rate, $G(D)$ can be expressed in terms of the overall polymerization rate for each class of particles, $R_p(D)$, as follows:

$$G(D) = 2 R_p(D) / \rho_p \pi D^2 \tag{17}$$

The population balance equation has to be solved numerically using an accurate and efficient discretization method. In the present study, the orthogonal collocation on finite elements method

(OCFE) was employed for solving the dynamic PBE (Alexopoulos et al., 2004).

In an FBR solid mixing is induced by fast moving gas bubbles. A rising bubble drags solid particles from the bulk emulsion phase, while solids are moving from wake to the bulk phase at the same time, indicating that there is a continuous interchange of particles between the two phases. It is obvious that the development of a correlation is required to describe correctly the type of particles that are entrained by the bubbles. According to Choi et al. (2001), the following empirical exponential correlation can be applied in order to calculate the particle transfer constant from bulk to wake phase.

$$k_{tr}^{bw}(D) = A\rho_g \exp(-u_t/u_0) \qquad (18)$$

where ρ_g is the density of fluidizing gas, u_0 is the superficial gas velocity, u_t is the terminal velocity and A is an adjustable parameter (A = 0.0658). Notice that the particle transfer rate constant from bulk phase to wake becomes size dependent because the terminal velocity is size dependent.

Finally, the number- and weight- average molecular weights for all particles in the reactor will be given by the weighted sum of mean-average molecular weights calculated in the particle level (i.e., $M_n(D)$, $M_w(D)$) with respect to the particle size distribution.

$$M_{n,bed}(t) = \int_{D_{min}}^{D_{max}} M_n(D)p_p(D,t)dD \qquad (19)$$

$$M_{w,bed}(t) = \int_{D_{min}}^{D_{max}} M_w(D)p_p(D,t)dD \qquad (20)$$

where $p_p(D,t)dD$ denotes the mass fraction of particles in the size range (D to $D+dD$) at time t per mass of polymer in the bed.

Table 2 Nominal operating conditions and numerical values of the physical and transport properties of the reaction mixture

Reactor Operating Conditions	Physical Properties
W (kg) = 64177	ΔH_r (J/g) = -3832
F_c (g/s) = 0.1	$\rho_{g,1}$ (kg/m^3) = 28
D_c (μm) = 50	$\rho_{g,2}$ (kg/m^3) = 42
T_b (K) = 353.15	$\mu_{g,1}$ (Pa·s) = 1.2×10^{-4}
$[M_1]_b$ (mol/L) = 0.65	$\mu_{g,2}$ (Pa·s) = 10^{-4}
$[M_2]_b$ (mol/L) = 0.15	$D_{b,1}$ (cm^2/s) = 0.006
$[H_2]$ (mol/L) = 0.03	$D_{b,2}$ (cm^2/s) = 0.004
$[Coc]$ (mol/L) = 0.01	

5. RESULTS AND DISCUSSION

Extensive numerical simulations were carried out by using the proposed model (see to Figure 1) to investigate the effects of various reactor operating conditions on the distributed molecular and morphological polymer properties in a catalyzed, gas phase, ethylene propylene copolymerization FBR. The reactor operating conditions and the numerical values of the physical and transport properties of the reaction mixture are reported in Table 2.

In Figure 2, the effect of fluidization gas velocity on the particle size distribution in the reactor compartments is shown. In the present multi-compartment model the number of compartments was set equal to five through all model simulations. For illustration purposes the PSDs in the top, bottom and in an intermediate compartment are shown. As can be seen, at low gas velocities, the PSD is shifted to larger sizes from the top to bottom compartment, according to the general segregation pattern. As the gas velocity increases, the individual PSDs in each compartment collapse into the same distribution, implying that the FBR can be approximated by a single CSTR.
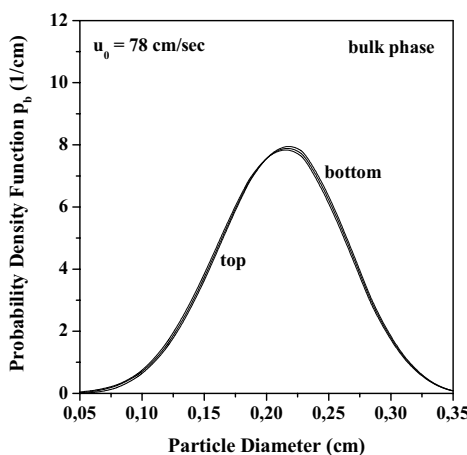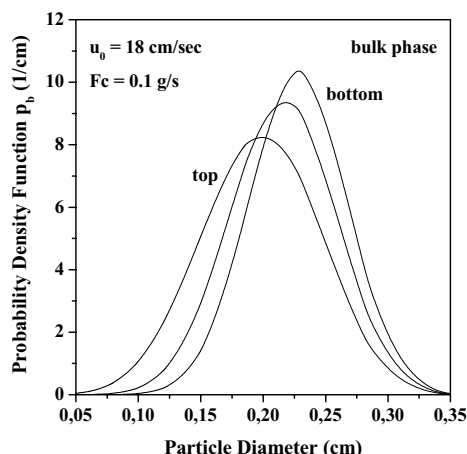
Fig. 2. Effect of fluidization gas velocity

The particle size distributions in the wake phase are shown in Figure 3. As expected, the amount of small particles in the wake phase is substantially larger

than in the bulk phase, which is correct because as a bubble rises in the reactor carries particles small in size.
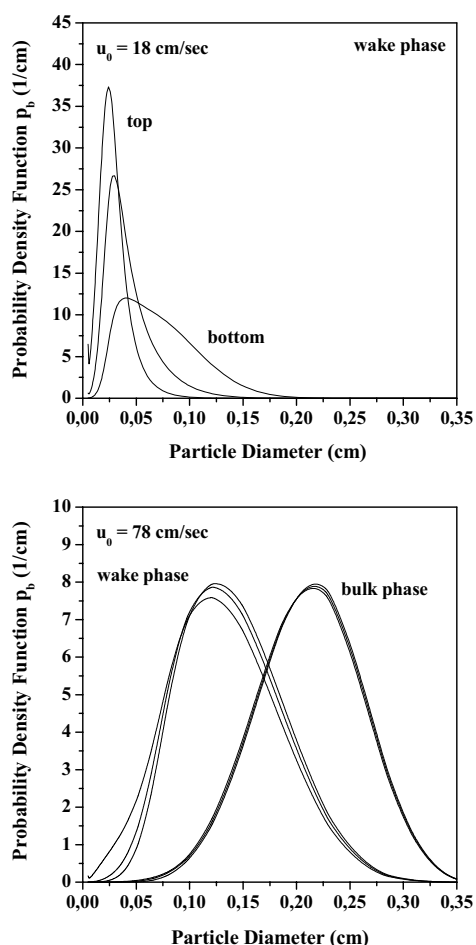
Fig. 3. Effect of fluidization gas velocity.

In Figure 4, the dynamic evolution of ethylene concentration in the reactor is depicted for different fluidization gas velocities. According to this Figure, as the gas velocity increases less monomer is consumed because its conversion is relatively low.
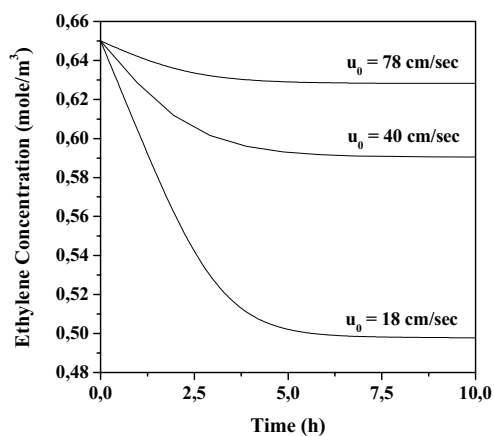
Fig. 4. Effect of fluidization gas velocity on ethylene consumption in the reactor.

In Figure 5, the effect of catalyst feed rate is shown. It is apparent that as the catalyst feed rate increases,

the polymer particle size distribution becomes narrower and is shifted to smaller sizes. It is important to point out that as the catalyst feed rate increases, more particles grow in the bed and because the bed weight is kept constant, the residence time of particles in the reactor decreases. As a result the amount of large polymer particles in the reactor decreases.
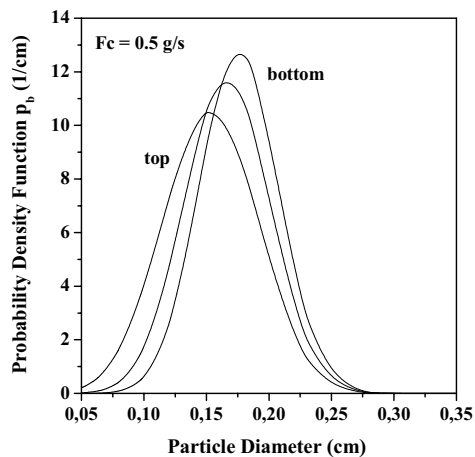
Fig. 5. Effect of catalyst feed rate

In Figure 6, the dynamic evolution of the average particle size of the distribution in the reactor for the two catalyst feed rates studied brfore, is depicted. It is obvious that as the catalyst feed rate decreases the time required for the PSD to reach its final steady-state value increases.
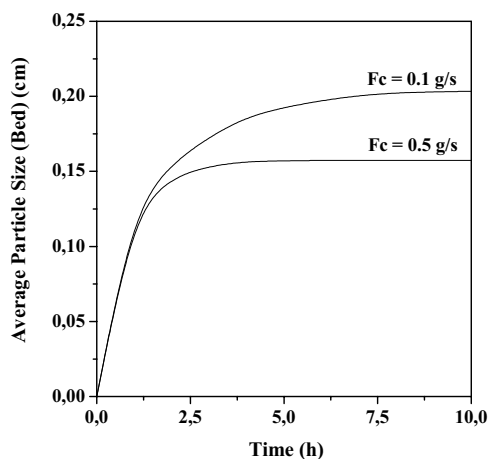
Fig. 6. Effect of catalyst feed rate on the average particle size of the PSD in the reactor.

In Figure 7, the effect of catalyst feed rate on the dynamic evolution of the polymer weight average molecular weight in the reactor compartments is illustrated. According to the results of this Figure, an increase of catalyst feed rate significant affects the WAMW of polymer produced during the dynamic operation of the reactor. Particles in the upper compartment due to their smaller size require less time for their PSD to reach its steady-state value. As a result the time required for their molecular weight to reach its steady state value, is also smaller in

comparison with the corresponding time of particles existed in lower compartments. That is the reason why for a certain time instant more WAMW is produced in the top compartment. Also can be seen, that a steady state WAMW value is achieved after approximately 4 hours, when the catalyst feed rate is equal to 0.5g/s, and 10 hours, when the catalyst feed rate is equal to 0.5g/s, respectively.
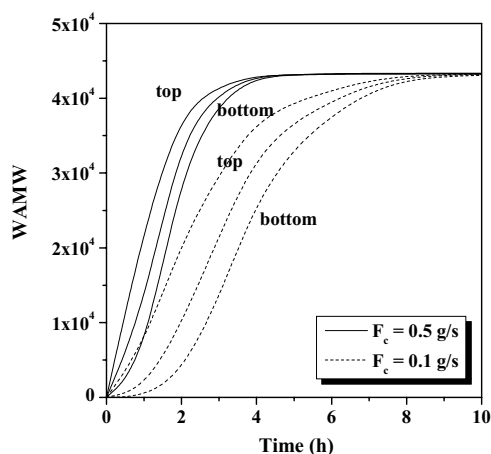
Fig. 7. Effect of catalyst feed rate on the dynamic evolution of the polymer weight average molecular weight in the reactor compartments.

6. CONCLUSIONS

In the present study, a comprehensive multi- scale, multi-compartment dynamic model is developed to analyze the dynamic behavior of fluidized bed reactors for ethylene-propylene copolymerization through mathematical modeling and simulation. The model can also be used for the prediction of morphological (i.e., particle size distribution (PSD) and particle segregation) as well as molecular (i.e., molecular weight distribution (MWD)) distributed polymer properties in a catalytic olefin polymerization FBR. It is illustrated that at low fluidization gas velocities particle segregation phenomena become significant and may influence the morphological and molecular properties of polymer particles in the bed. Although no actual experimental data are reported in the open literature regarding segregation phenomena in industrial fluidized bed reactors, our model results are in qualitative agreement with industrial observations.

REFERENCES

Alexopoulos, H.A., A.I. Rousos and C. Kiparissides (2004). Part 1: Dynamic evolution of the particle size distribution in particulate processes undergoing combined particle growth and aggregation. . *Chemical Engineering Science*, 59, 5751-5769.

Choi, K.Y., X. Zhao and S. Tang (1994). Population balance modelling for a continuous gas phase olefin polymerization reactor. *Journal of Applied Polymer Science*, 53, 1589-1597.

Dompazis, G., V. Kanellopoulos and C. Kiparissides (2005). A multi-scale modeling approach for the prediction of molecular and morphological properties in multi-site catalyst, olefin polymerization reactors. *Macromolecular Materials and Engineering*, 290, 525-536.

Hatzantonis, H., A. Goulas, and C. Kiparissides (1998). A comprehensive model for the prediction of particle-size distribution in catalyzed olefin polymerization fluidized-bed reactors. *Chemical Engineering Science*, 53, 3252.

Hatzantonis, H., A. Yiagopoulos, H. Yiannoulakis and C. Kiparissides (2000). Recent developments in modeling gas-phase catalyzed olefin polymerization fluidized-bed reactors: The effect of bubble size variation on the reactor's performance. *Chemical Engineering Science*, 55, 3237-3259.

Kanellopoulos, V., G. Dompazis, B. Gustafsson and C. Kiparissides (2004). Comprehensive analysis of single-particle growth in heterogeneous olefin polymerization: the random-pore polymeric flow model. *Ind. Eng. Chem. Res.*, 43 (17), 5166-5180.

Kim, J.Y. and K.Y. Choi (2001). Modeling of particle segregation phenomena in a gas phase fluidized bed olefin polymerization reactor. *Chemical Engineering Science*, 56, 4069-4083.

Yiannoulakis, H., A. Yiagopoulos and C. Kiparissides (2001). Recent developments in the particle size distribution modeling of fluidized-bed olefin polymerization reactors. *Chemical Engineering Science*, 56, 917-925.

Zacca, J.J., A.J. Debling and H.W. Ray (1996). Reactor residence time distribution effects on the multistage polymerization of olefins I. Basic principles and illustrative examples, polypropylene. *Chemical Engineering Science*, 51 (21), 4859-4886.